Detection and Evaluation of Driver Distraction Using Machine Learning and Fuzzy Logic

Andrei Aksjonov, Pavel Nedoma, Valery Vodovozov, Eduard Petlenkov, and Martin Herrmann

Abstract—**In addition to vehicle control, drivers often perform secondary tasks that impede driving. Reduction of driver distraction is an important challenge for the safety of intelligent transportation systems. In this paper, a methodology for detection and evaluation of driver distraction while performing secondary tasks is described and an appropriate hardware and software environment is offered and studied. The system includes a model of normal driving, a subsystem for measuring the errors from the secondary tasks, and a module for total distraction evaluation. A new machine learning algorithm defines driver performance in lane keeping and speed maintenance on a specific road segment. To recognize the errors, a method is proposed, which compares normal driving parameters with ones obtained while conducting a secondary task. To evaluate distraction, an effective fuzzy logic algorithm is used. To verify the proposed approach, a case study with driver-in-the-loop experiments was carried out, in which participants performed the secondary task, namely chatting on a cell phone. The results presented in this research confirm its capability to detect and to precisely measure a level of abnormal driver performance.**

Index Terms—**Euclidean distance, fuzzy logic, fuzzy neural networks, machine learning, prediction method, vehicle safety.**

I. Introduction

A driver is the most important participant of a car control, including steering, throttling, braking, maneuvering, and other operations. These primary tasks must be accomplished safely for all traffic participants and their belongings.

Nevertheless, drivers often dedicate time and attention to other activities, different from the driver's primary ones. All other tasks the drivers perform while driving are defined as secondary tasks. They are divided into interaction with in-vehicle information systems (IVIS) (e.g. monitoring and managing vehicle state, navigating, info- and entertainment, etc.) and interaction with personal (e.g. passengers and pets) or items brought in a vehicle, such as portable electronic devices [1, 2].

Driver distraction (DD) is defined as *an activity performed by a driver that diverts an attention away from the primary activity (vehicle longitudinal and lateral control) potentially leading to safe driving degradation. It appears due to some event, activity, object, or person within or outside the vehicle, which compels or induces the driver's attention away from the primary task* [1]. With an enhancement of IVIS, driving comfort, entertainment, and navigation have dramatically improved. However, at the same time, IVIS attracts additional driver's attention. It increases DD, what often leads to traffic accidents with fatal consequences. Yearly, distracted driving leads to more than 420000 injuries. Furthermore, the number of drivers end abruptly in vehicle crashes due to DD is more than 3100 every year in the USA alone [3].

DD may take several forms: auditory, biomechanical, cognitive, or visual [1, 3]. Auditory distraction means taking ears off the road (e.g. listening to the radio or passengers). Biomechanical one is taking hands off the steering wheel (e.g. eating, texting messages, IVIS adjusting). Cognitive distraction means taking mind off the road (e.g. thinking, talking). Visual distraction is caused by taking eyes off the road (e.g. reading, watching video, road navigating in IVIS). However, most of the secondary tasks take more than one if not all the distraction forms simultaneously [1, 4], those tasks are among the most dangerous [3]. Texting, for instance, requires manual, visual and cognitive distraction types at once, when the last one is considered as the most essential [3].

Research in driver's decoy caused by the secondary activity, especially by IVIS, arises a great interest of both the vehicle manufacturers and the traffic safety foundations, like the American Automobile Association (AAA) Foundation for Traffic Safety (Washington, DC, USA) and National Highway Traffic Safety Administration (NHTSA) (Washington, DC, USA). It helps to establish traffic safety policies, to contribute to the design, and to improve IVIS, which must be safe, intuitive, reachable, logic, and well organized to decrease driver's workload and disturbance and, consequently, to increase traffic safety.

Therefore, a development of a robust DD detection and evaluation method while performing a secondary task is a significant target in safe intelligent transportation. It gives an

This project has received funding from the European Union's Horizon 2020 Research and Innovation program under grant agreement No. 675999.

A. Aksjonov and P. Nedoma are with the ŠKODA AUTO a.s., Mladá Boleslav, 29301 Czech Republic (e-mails: andrei.aksjonov@skoda-auto.cz; pavel.nedoma@skoda-auto.cz).

V. Vodovozov is with the Department of Electrical Power Engineering and Mechatronics, Tallinn University of Technology, Tallinn, 19086 Estonia (e-mail: valery.vodovozov@ttu.ee).

E. Petlenkov is with the Department of Computer Systems, Tallinn University of Technology, Tallinn, 19086 Estonia (e-mail: eduard.petlenkov@ttu.ee).

M. Herrmann is with the IPG Automotive GmbH, Karlsruhe, 76185 Germany (e-mail: martin.herrmann@ipg-automotive.com).

opportunity to study and to compare several types of human-machine interaction (HMI) technologies (e.g. haptic, vocal, gesture) and to use the most appropriate one in IVIS design. DD assessment is also applied in advanced driver assistance systems (ADAS) and in testing and evaluating their impact on driver's level of vigilance and road safety. Today, there are no estimates for evaluating the influence of the secondary tasks on DD that might indicate the secondary activities that lead to potential traffic accidents, assess a degree of their danger, and help mitigate these effects [1].

The goal of the current study is to develop a method of evaluating a secondary task impact to the safe vehicle operation suitable for DD detection, DD level measurement, and comparison of the secondary tasks influence on DD. The method is exploited as a benchmark for safe and clear IVIS design with minimal driver's burden in different HMI technologies (e.g. voice command, hand gesture recognition).

This paper is organized as follows. The next section presents the state of the art of DD detection relevant for current studies. Section III is dedicated to the description of the DD evaluation methodology. The real-time driver-in-the-loop DD experiment is described in Section IV. Section V outlines the experimentally obtained results. The research is concluded in Section VI.

II. Related Works and Problem Statement

In general, there are four attributes suitable for DD measurement and detection: behavioral (e.g. eye and head movement); performance-based (e.g. vehicle lateral and longitudinal control); psychological (e.g. driver electrocardio– and electroencephalographical methods), and subjective (e.g. self–assessment questionnaires and expert evaluations). The first two are the most frequently used ones. Different attributes can be also combined [5, 6, 7].

On the other side, a variety of algorithms has been offered for the DD detection based on statistical learning theory. The gaze direction and the head orientation are the most popular input attributes [8]. Artificial neural network (NN) and gradient boosting machine combination were proposed in [9]. The glance region prediction algorithm was designed using random forest classifier in [10] and convolutional NN – in [11]. In [12], dynamic Bayesian network (BN) outperformed logic regression (LR), static BN, and support vector machine (SVM) approaches in cognitive DD detection. SVM together with semi-supervised extreme learning machine were combined for the DD detection in [5]. Classification based on Mahalanobis distance calculation was applied for the evaluation of IVIS-induced DD in real-time [13]. Fuzzy expert system combined eye and face regions for the DD level fatigue estimation in [14]. Different machine learning methods, in particular SVM, *k*-nearest neighbor (*k*-NN), and graph-regularized extreme learning machine were compared in [15]. The complex method designed in [7] connects the principle component analysis, the linear discriminate analysis, and SVM. Finally, in [16], a probabilistic restricted Coulomb energy NN was implemented for drowsy driving prediction.

Multiple psychological attributes were also studied for the DD detection. In [6], the brain activity measured by electroencephalographic signals was involved to predict the start and the end of a distraction period using an adaptive-threshold-based prediction framework. In [17], the same signal analyses were applied for the DD detection by different machine learning methods: decision tree, random forest, *k*-NN, SVM, and Naïve Bayes. The driver drowsiness detection using heart rate electrocardiogram signals with LR and BN was described in [18].

Very popular is the usage or performance-based attributes in the DD detection as an estimate of the vehicle dynamics. As the signals are received here from the sensors available in modern passenger vehicles [19], this approach does not require any additional hardware.

An example of the DD detection usage in ADAS is described in [20]. The scholars presented fuzzy system, which personalizes the fuzzy membership functions based on individual driving habits. The system reflects user's preferences in the cruise control. Vehicle performance-based data were used in the fuzzy system design.

The DD detection with artificial NN and Gaussian mixture model (GMM) using performance-based attributes was introduced in [21] and [22]. The double-class DD classifier based on GMM was described in [23]. Vehicle dynamics and driving performance results were engaged in the DD detection by an extreme learning machine algorithm in [24] and SVM – in [2]. In [25], authors presented the driver behavior prediction with dynamic BN based on preliminary collected data.

Since 1999, on-road data of drivers were collected for their further study in [26]. Statistical signal processing and machine learning techniques, such as GMM, hidden Markov model (HMM), and BN were applied to simulate such aspects of driver's behavior like pedal orientation, car following, and lane change. These data were successfully used for predicting the driver behavior and detecting risky driver frustration.

Many different DD detection algorithms, namely static and dynamic NN, adaptive neuro-fuzzy inference system (ANFIS), and SVM, were compared in [27]. The last one outperformed all other machine learning methods used in the work.

Lastly, different DD detection attributes, like performance-based, psychological, and behavioral, were combined. A gaze angle, a head rotation angle, and an interval between the heart R-wave electrocardiogram signals were used in cognitive DD [28], where the pattern recognition methods based on SVM and adaptive boosting were compared. The last one showed better accuracy. In [29], the control theoretic driver model based on the literary physiological aspect was induced by the driver's behavior predictive model design. This model was compared with a real driver performance.

The driver's eye movement and vehicle performance were integrated as a real-time cognitive DD attribute [4, 30, 31] and the SVM algorithm was applied in these studies. Driving performance and head movement tracking were integrated for the DD detection with random forest model and HMM [32]. In [33], different machine learning methods, SVM, conventional recurrent NN, and long or short-term memory recurrent NN, using the same attributes were compared for continuously driver's state prediction. The last one was more accurate in classification. In [34], DD prediction based on ANFIS was compared with the artificial NN and radial basic function prediction algorithms. The results proved that ANFIS has more accurate prediction capability. Driver performance along with heart rate and behavioral attribute data were combined for the DD and fatigue detection in [35]. Classification was performed by a multi-modal approach based on HMM, SVM, and BN.

Though the physiological and behavioral attributes represent a trend in DD detection, they always require additional devices, such as cameras and neuroscan systems that multiply system cost and complexity [8]. Moreover, often wearing devices, like eye-tracking googles or neuroscan helmets, are considered as a distraction source themselves. Then, some scholars consider the behavioral methods as the only capable to detect visual DD. Eye and head movement tracking are not qualified to observe driver's cognitive workload, such as talking to a passenger. It is unknown, how a cognitive distraction depends on eye and head movement required for the primary task performance [4, 27, 30]. This is the reason why the vehicle dynamic performance (center-lane driving and vehicle speed limit maintenance) has been chosen as a driver's primary task in this study.

Despite a variety of machine learning algorithms proposed for the DD detection, all of them use the Boolean binary classification (distracted/not distracted). These solutions are not suitable for different HMI technologies for accurate IVIS comparison. Never approaches have been found for accurate measuring of a DD level, especially in applying the performance-based attributes while interacting with IVIS.

The target of this paper is to propose a method, which not only detects, but also evaluates a DD level of each individual driver considered as an essential task of the safe IVIS design. To this aim, a regression problem of the DD detection is solved aiming to form the output as a precise number [36] using the machine learning approach. Thanks to accurate measurement, the level of the secondary task influences on the driver's performance is evaluated here. Nonlinear regression based on Euclidean distance (ED) calculation is applied for the DD detection. Fuzzy logic (FL) is used for fusion of vehicle performance data to assemble a level of DD from two independent variables. The driver-in-the-loop experiment on DD detection and evaluation was conducted, in which text messaging on a cell phone has been chosen as a secondary distractive activity required several modes of distraction simultaneously [3]. In this way, a difference in vehicle performance at normal driving (fully dedicated to a primary activity) and accomplishing a secondary task while driving was observed aiming to estimate a personal degree of the secondary tasks influence on driving [2].

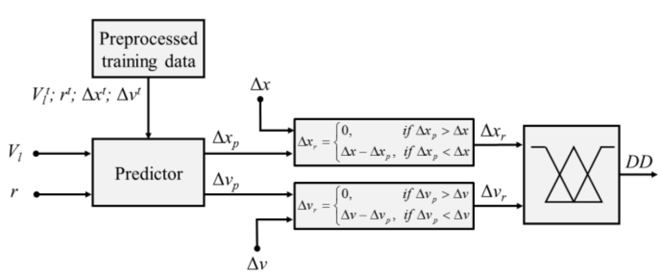

Fig. 1. DD detection and evaluation block scheme. Parameters description is presented in Table I.

Vehicle dynamics highly depend on the driver experience [35]. By this reason, a model of driver performance is created, which is assumed as a normal driving for each experiment participant. Next, the driving destructive performance is compared with normal driving in the real-time driver-in-the-loop experiment. To predict driver's normal performance, a regression-based machine learning algorithm is developed for participants' data collecting during a free run. In this paper, a technique that solves a regression problem and predicts driver performance on a specific road segment is defined as a predictor. What is more, as an ANFIS has very accurate prediction capability [27], the prediction approach based on ED formula is compared to an identical ANFIS predictor.

Next, the driving performance data are merged into a uniform variable, which represents a percentage level of DD caused by the secondary task. To this aim, the FL method is used. Among the most popular signal fusion techniques – FL, BN, and machine learning – FL is known as a perfect approach for empirical modeling of human behavior reasoning, because it simultaneously concerns several vague inputs, and for the vigilance information fusion [35, 37].

III. Description of the Method

A scheme of the DD detection and evaluation is shown in Fig. 1. The symbols' description and annotation are introduced in Table I. The superscript "*t*" determines "training data".

The method involves three steps. First, referring to a road segment specification (road curvature r and speed limit V_l), it predicts driver's ability to keep the centerline Δx_p and to maintain the speed limit Δv_p. The predictor is trained preliminary without secondary activity for every driver, and training data are collected. Second, the predicted driver performance is compared with a performance with the secondary task Δx and Δv. As a result, their differences Δx_r and Δv_r are calculated. Finally, the FL evaluator using linguistic rules normalizes two independent variables into a uniform variable DD, which designates the DD level in percentage.

A. Prediction of driver performance based on Euclidean distance calculation

To create a prediction model for an individual driver, he/she must drive a road segment without a distraction. During this run, the driver is asked to demonstrate an accurate performance:

TABLE I
Parameters Description

Symbol	Description	Unit
r	Road radius (curvature)	m
V_l	Speed limit	km/h
Δx	Real lane keeping offset	m
Δv	Real vehicle speed deviation	km/h
Δx_p	Predicted lane keeping offset	m
Δv_p	Predicted vehicle speed deviation	km/h
Δx_r	Resultative lane keeping offset	m
Δv_r	Resultative vehicle speed deviation	km/h
DD	Driver distraction level	%

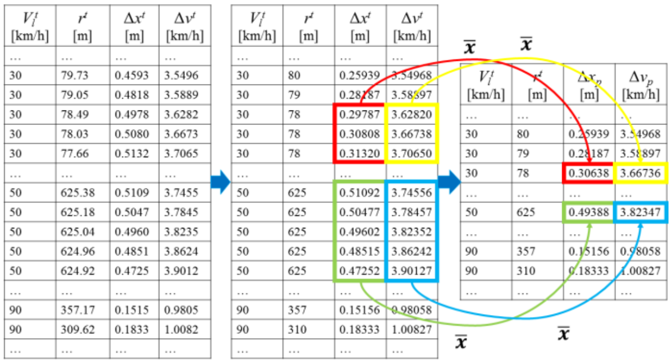

V_l^t [km/h]	r^t [m]	Δx^t [m]	Δv^t [km/h]
...	...	...	...
30	79.73	0.4593	3.5496
30	79.05	0.4818	3.5889
30	78.49	0.4978	3.6282
30	78.03	0.5080	3.6673
30	77.66	0.5132	3.7065
...	...	...	...
50	625.38	0.5109	3.7455
50	625.18	0.5047	3.7845
50	625.04	0.4960	3.8235
50	624.96	0.4851	3.8624
50	624.92	0.4725	3.9012
...	...	...	...
90	357.17	0.1515	0.9805
90	309.62	0.1833	1.0082
...	...	...	...

V_l^t [km/h]	r^t [m]	Δx^t [m]	Δv^t [km/h]
...	...	...	...
30	80	0.25939	3.54968
30	79	0.28187	3.58897
30	78	0.29787	3.62820
30	78	0.30808	3.66738
30	78	0.31320	3.70650
...	...	...	...
50	625	0.51092	3.74556
50	625	0.50477	3.78457
50	625	0.49602	3.82352
50	625	0.48515	3.86242
50	625	0.47252	3.90127
...	...	...	...
90	357	0.15156	0.98058
90	310	0.18333	1.00827
...	...	...	...

V_l^t [km/h]	r^t [m]	Δx_p [m]	Δv_p [km/h]
...	...	...	...
30	80	0.25939	3.54968
30	79	0.28187	3.58897
30	78	0.30638	3.66736
...	...	...	...
50	625	0.49388	3.82347
...	...	...	...
90	357	0.15156	0.98058
90	310	0.18333	1.00827
...	...	...	...

Fig. 2. Training data dimensional reduction.

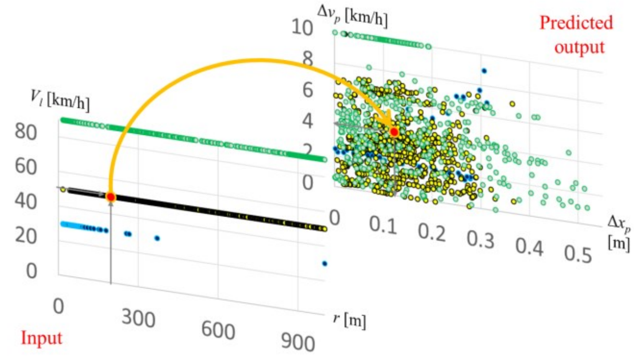

Fig. 4. Visual explanation of driver performance prediction using Euclidean distance formula.

to obey the speed limits and to keep the middle lane of the road as perfectly as possible. The predictors' training data include four variables: speed limit V_l^t; radius of the road r^t; lane keeping offset Δx^t; vehicle speed deviation from a speed limit Δv^t. The first two variables are related to the road information whereas two others – to driver performance. Thus, a map of driver performance is created on each specific road segment, described by the road curvature (radius) r and speed limit V_l.

Further, the obtained data are passed through preprocessing (dimensional reduction), during which this training information is diminished or simplified to reduce memory, computation, and inference complexity. Besides, the model simplification makes the method more robust, understandable, and easy to plot and analyze. There exist some preprocessing algorithms, such as the subset selection, the principle components analysis, the factor analysis, etc. [23, 36]. An approach used in this study is described below.

First, the training data are stored in a table. Second, the radiuses of the road segments are rounded to the whole numbers. Third, the unique pairs of a road curvature and a speed limit are found. Finally, a mean offset between the road centerline and a position of the car on the road, and a mean difference between the speed limit on a road segment and a real vehicle speed for each unique pair of road information are calculated. This preprocessing allows shrinking significantly the size of the data sample. For instance, the data collected during the 20-minute driving consisted of about 50 000 nodes. After preprocessing, these data shrank to 10% of total points.

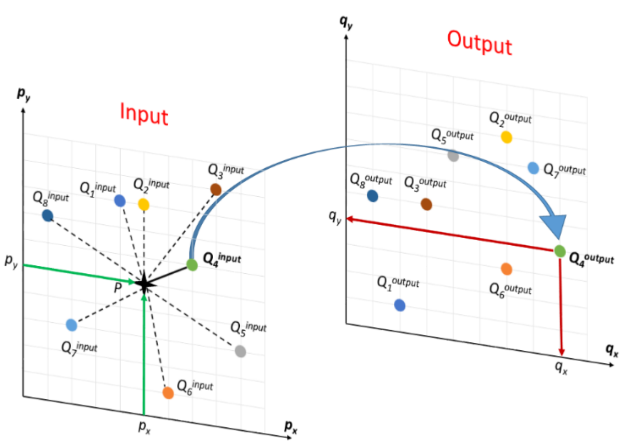

Fig. 3. Visual explanation of predicted value search based on Euclidean distance calculation.

Described preprocess steps separated with blue arrows are shown in Fig. 2.

Consequently, the data table is obtained where every possible pair of input variables (road information) corresponds to a pair of output variables (driver performance). The outputs symbolize an average lane keeping and speed limit maintenance ability for a specific road segment. Input/output mapping is fulfilled with ED calculation.

During the experiment with the secondary activity, the information about the road segment is inserted into a prediction block containing preprocessed training data (Fig. 1). The predictor inputs are the real-time speed limit V_l and road radius r. The Input road information is aligned with unique pairs of the road set from the data table. The ED function $d(P,Q)$ is used to search a closest pair of the prediction model input sets:

$$d(P,Q) = \sqrt{\sum_{i=1}^{k} (q_i - p_i)^2}\,, \tag{1}$$

where k is a spatial dimension.

The predicted searching procedure with ED calculation is simplistically illustrated in Fig. 3. Assume that P is a point with coordinates ($p_x = r$, $p_y = V_l$). Points Q_n^{input} have coordinates ($q_{xn}^{input} = r_n^t$, $q_{yn}^{input} = V_{ln}^t$) from the training data table, where n is a row number in the table. All the distances are calculated between a single input point P and each point Q_n^{input} from the table with simplified training data. A set of point coordinates Q_n^{input} with the shortest distance between P and Q_4^{input} in Fig. 3 is accepted as possible driver performance on a road segment and returns the predicted output values ($q_{xn}^{output} = \Delta x_{pn}$, $q_{yn}^{output} = \Delta v_{pn}$) that correspond to their row in the table.

A predictor input and output pair matching is depicted in Fig. 4. The input and output values are presented in separate Cartesian coordinate systems. Each coordinate in the first system has a unique pair of the coordinates in the parallel two-dimensional one. By finding the nearest set of trained input, the possible output is predicted and stored in the parallel coordinate system. Accordingly, possible driver performance is estimated, in a name of lane keeping and speed maintenance, on each road segment given by its speed limit and curvature.

Next, as it is also seen in Fig. 1, driver predicted performances Δx_p and Δv_p are compared with the real ones Δx and Δv using the following rules:

$$\Delta x_r = \begin{cases} 0, & \text{if } \Delta x_p > \Delta x \\ \Delta x - \Delta x_p, & \text{if } \Delta x_p < \Delta x \end{cases}, \tag{2}$$

$$\Delta v_r = \begin{cases} 0, & \text{if } \Delta v_p > \Delta v \\ \Delta v - \Delta v_p, & \text{if } \Delta v_p < \Delta v \end{cases}. \tag{3}$$

More precisely, if a predicted value is higher than a real value, the algorithm sends zero as a system output. It means that driving is normal for the current driver. When a predictive value is smaller than a real value, the difference between two values is calculated and assigned as a system output. Hence, a hypothesis is posed that when the driver performance becomes worse due to distraction, the algorithm detects unusual vehicle dynamic performance. Finally, the obtained lane keeping offset Δx_r and speed difference Δv_r serve as the inputs to the FL reasoning to evaluate a level of distraction.

B. Driver performance prediction with an adaptive neuro-fuzzy inference system

To study the degree of accuracy of the prediction method described in the previous subsection, an ANFIS prediction model has been designed for a driver. Therefore, the ED and ANFIS predictors are compared during driver-in-the loop experimentation.

ANFIS is a feedforward five-layer network with supervised learning capability. It is functionally equivalent to a first-order Sugeno's fuzzy model. To support both the batch (off-line) and the pattern (on-line) learning, ANFIS combines least–squares estimator and the gradient descent method as training algorithms. During the single training epoch, ANFIS applies both the forward and the backward passes [38]. Significant improvement in ANFIS performance accuracy can be achieved with a greater number of membership functions (MFs) for the prediction model rather than an increasing number of training epochs [36]. In our case, trained ANFIS is integrated with the real-time experiment identically to the ED predictor. The same training data without preprocessing as in the ED predictor are utilized in ANFIS training. MATLAB® Fuzzy logic Toolbox™ from MathWorks, Inc. (Natick, Massachusetts, USA) is used to design an ANFIS predictor for each experiment participant.

The difference in accuracy at applying 5, 50 or even 100 epochs is not sensitive [38]. The minimum possible for current training data set sum of squared errors was obtained with five MFs for every input variable. Hence, the network generates 25 rules, what took only three epochs. As suggested in [38]: 70% of sample data were used for training, 15% – for testing and the rest – for validation.

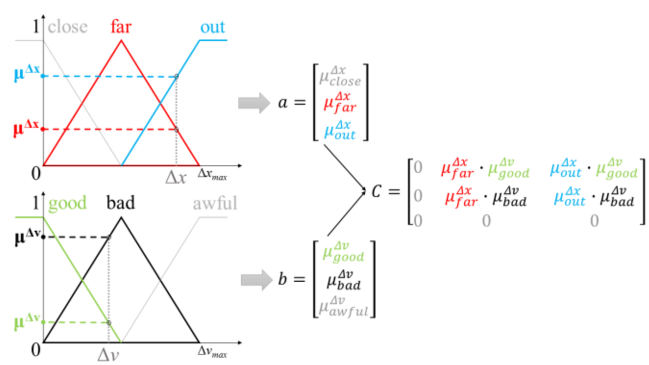

Fig. 5. Fuzzification procedure.

When the secondary task experiment is performed, the ANFIS model receives the same information about the road as the ED predictor. The outputs of ANFIS represent the driver performance predictions Δx_p and Δv_p. Thus, two equivalent predictors are trained with the same data to compare.

C. DD evaluator with FL

FL system design includes four stages: fuzzification, inference engine, rule-base, and defuzzification. It may have many inputs and outputs represented the real numbers. The first stage in fuzzy reasoning is a fuzzification, where each real number on the input is transformed into a fuzzy set, that is a pair consisting of an element in universe of discourse (UOD) and a degree of certainty of MF. The rule-base stores linguistic rules and is exploited to match fuzzy input with fuzzy output sets via an inference mechanism. Finally, a defuzzification procedure transforms fuzzy output sets back to real numbers [37].

In [39], a fuzzy inference process based on simple matrix operations is introduced. In the current study, the same approach is used for FL evaluator design. It has two inputs: an offset of the car position on the road Δx_r from the road centerline and a difference between the speed limit on a road segment and a real vehicle speed Δv_r. The inputs are generated during the driver prediction and real-time performance comparison described previously.

Both inputs Δx_r and Δv_r have symmetrically dispersed triangular MFs, what guarantee fast response and equal sensitivity of the input variables [37]. MFs are overlapped over the whole UOD. The Δx_r is restricted to [0 1.5]. The UOD of the Δv_r is narrowed in [0 12].

The inputs are transformed into appropriate column vectors a and b, those elements are equal to a degree of certainty of a relevant MF. MFs that are not crossed by the input variable are equal to 0. Every input has three MFs. Therefore, the fuzzified column vectors have the size of 3x1. The dyadic product of obtained vectors generates a 3x3 matrix $C = ba^T$. Each element of the generated matrix C is a real number between zero and one. The fuzzification process together with the designed MFs is shown in Fig. 5.

The FL rule-base stores the linguistic rules relation between the input and output MFs. The linguistic knowledge is expressed in modes-ponens-form rules "If-Then". As the system has two inputs and one output, nine rules are designed in total for the FL evaluator. The rule-base is presented in Table II, where the MFs are named suitably for human understanding. The distance from a vehicle and road centerline Δx_r consists of 3 levels: "*close*" (to the centerline), "*far*" (from the centerline) or "*out*" (of the road bounds). The ability of the speed limit maintenance Δv_r is defined as "*good*", "*bad*" or "*awful*". An

TABLE II
RULE-BASE OF THE FL EVALUATOR

DD		Δx_r: close	far	out
Δv_r	good	*no*	*negligible*	*low*
	bad	*no*	*medium*	*high*
	awful	*very_low*	*very_high*	*inacceptable*

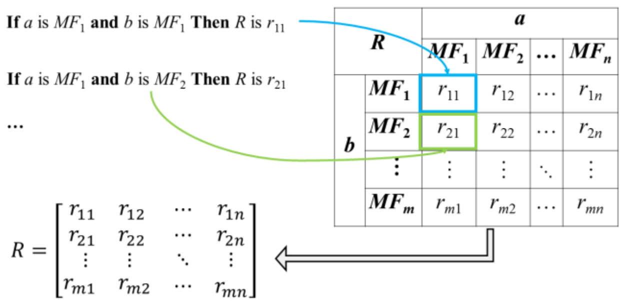

Fig. 6. Transformation of a FL rule-base into an $m \times n$ matrix.

example of the linguistic rule meaning is as follows (Table II): **IF** the vehicle middle point is "*far*" from the road centerline **AND** driver's speed limit maintenance is "*awful*", **THEN** driver distraction is "*very_high*".

Next, this linguistic knowledge is represented as a 3×3 matrix *R*, the elements of which are the values of the output singleton MFs: {*no* = 0, *negligible* = 14.3, *low* = 28.6, *very_low* = 42.9, *medium* = 57.2, *high* = 71.5, *very_high* = 85.8, *inacceptable* = 100}. The FL output presents DD in percentage, where each MF has equal step between each other in the UOD from 0 to 100. In Fig. 6, the transformation from the FL linguistic knowledge into an $m \times n$ matrix *R* is shown. In our case, both *m* and *n* are equal to three.

After that, equally sized matrices *C* and *R* are multiplied with Hadamard product approach resulting in matrix $D = C \circ R$. Each element of *D* contains information about the certainty of each output MF activation for a specific input.

The last stage of the FL inference system is the conversion of fuzzy matrices back to a numerical value. This is done via one of the most popular defuzzification methods, center of gravity. To transform the matrices into a number, a weighted average of the matrix elements is found as the sum of the elements in matrix *D* divided by the sum of the elements in matrix *C*. The three-dimensional surface of the designed FL DD evaluator is observed in Fig. 7. The FL design specification is summarized in Table III.

TABLE III
FL SPECIFICATION

Parameter	Fuzzy logic evaluator
Structure	Multi-input, single-output
Crisp inputs	Δx_r = [0 1.5] (3 MFs) Δv_r = [0 12] (3 MFs)
Crisp output	*DD* = [0 100] (8 MFs)
Input membership functions	Triangular symmetric
Output membership functions	Singleton symmetric
Inference mechanism	Matrix (Sugeno's)
Rule-base	9 modes ponens
Defuzzification	Geometric center

IV. CASE STUDY

A. Participants

The participants of the driver distraction experiment were employees from IPG Automotive GmbH (Karlsruhe, Germany). All the participants (13 males and 5 females) took part in the experiment voluntarily. Their age ranged between 24 and 39 (mean 30.11) years. The participants' driving experience ranged between 1 and 21 years (mean 11.33).

Before the experiment, the drivers were questioned regarding the electronic devices, such as tablets, smartphones, laptops, e-readers usage while driving. Two participants admitted that they never use them while driving; two drivers noted that they use a device sometimes. Remaining drivers reported that they rarely use electronic devices. All the participants pointed out that they are aware about a danger of using devices while driving. After the experiment, the drivers also described their impression of distractive driving.

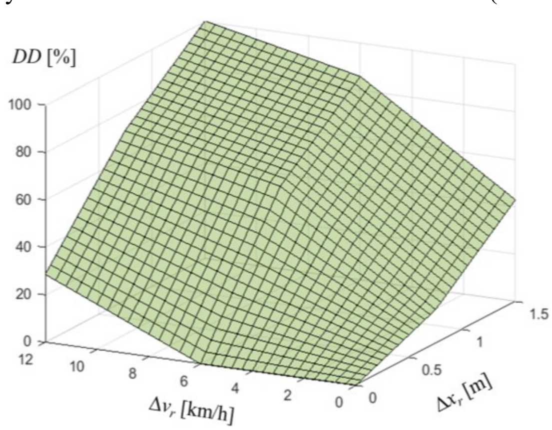

Fig. 7. Three-dimensional surface of the DD fuzzy evaluator.

B. Apparatus

The vehicle mockup driving simulator equipment System Experience Platform (SEP) is demonstrated in Fig. 8. The fixed-base test rig has a steering wheel and two pedals: acceleration and brake. SEP has an adjustable driver sit and two liquid-crystal displays. The virtual world is performed on a display placed in front of the driver. The virtual vehicle model has an automatic transmission. The vehicle speed is observable for the driver from the head-up display. The performance data are collected at a frequency of 50 Hz. The SEP supports MATLAB®/Simulink® (Natick, Massachusetts, USA) and IPG CarMaker® (Karlsruhe, Germany) real-time integration.

C. Procedure

The participants drove a two-way, two-line highway road of the total length of 10626 m and the line width of 3.5 m. The road had three segments with different speed limits (30, 50, and

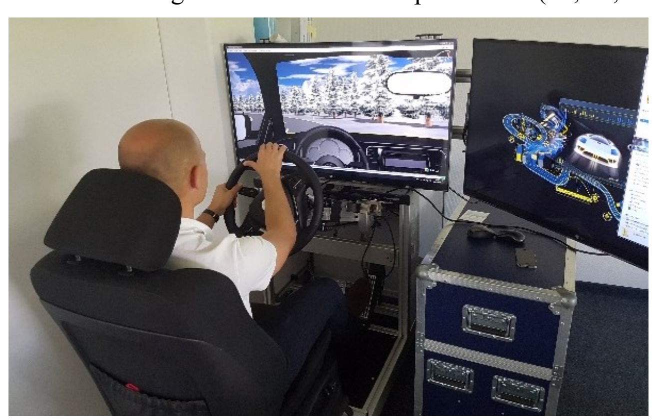

Fig. 8. SEP driving simulator.

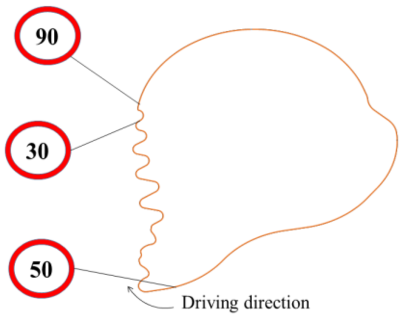

Fig. 9. Road shape with speed limits.

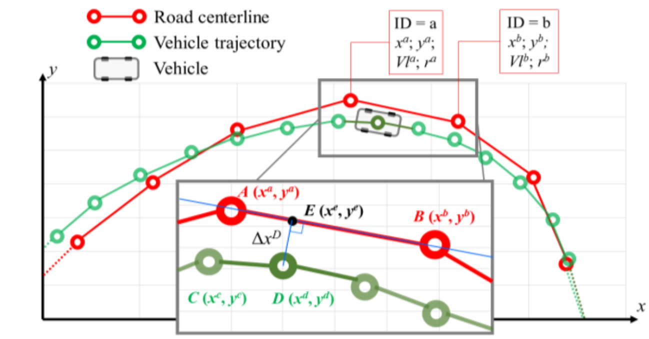

Fig. 10. Visual explanation of data extraction for point *D*.

90 km/h) and curvatures. The road shape along with the segments speed limits is plotted in Fig. 9. There were neither other vehicles or pedestrians nor animals modeled in the virtual world. Before the experiment, the drivers received unlimited time to familiarize themselves with the test rig and with the road. Moreover, during the experiment, the road shape and the vehicle location on the road were also displayed in the corner of one of the SEP's screens.

The first part of the experiment was dedicated to the data collection for ANFIS and ED predictors. Each participant passed two laps without a secondary task. They were asked to drive along the right side of the road and to respect all the traffic signs. The drivers were also informed, what data are used in driving prediction. After passing two laps, the participants continued driving one more lap, during which one of the experiment organizers sent text messages to the cellular phone prepared for the participants. The drivers were requested to answer the text messages and to continue driving respecting all the traffic rules. There was no time restriction for secondary task execution. The data collected in the third lap were used in the DD recognition.

The drivers were instructed to have a chat conversation naturally. The experimenter asked the participants simple questions, for instance "How are you?", "What are your plans for the weekend?" and similar. The secondary task period was captured since a driver took the phone in a hand and ending when the driver released the phone from the hands. The experimenter gave a reasonable time between the distractive messages. Therefore, each participant drove roughly equal time being distracted and being free from the secondary task.

D. Data extraction

The road consists of the nodes with fixed locations in Cartesian coordinate system, which are connected between each other with straight lines. Each node contains data {unique identification number (ID); x coordinate; y coordinate; speed limit V_l; road radius r}. During the experiment, the SEP saves the location of the vehicle geometric center in the virtual world with a fixed frequency.

In Fig. 10, an example of calculating Δx is illustrated. The red line symbolizes a road segment of the road curve (Fig. 9), while the green one - vehicle geometric center locations. In the point D of the vehicle trajectory with the coordinates (x^d, y^d), two nearest nodes A and B are searched from the road curve applying the ED function (1). Next, the shortest distance from the point D to the straight line between two nodes A and B is assigned as Δx^D. In Fig. 10, this shortest distance is the line DE.

The maximum speed in the point D is calculated using the coordinates of this point and the previous one C:

$$v^D = \frac{\sqrt{(x^d - x^c)^2 + (y^d - y^c)^2}}{\Delta t}\ , \tag{4}$$

where Δt is the time constant between data measurement for SEP. Finally, the speed deviation Δv^D for the point D is found as a difference between v^D and the speed limit V_l^a of the closest node A.

The road radius and speed limit for the point D are assigned from the closest of two nearest nodes of the road trajectory. In Fig. 10, the point D (green) passes the road segment characterized by the node A (red). Consequently, after data extraction, the point D includes attributes $\{\Delta x^D; \Delta v^D; V_l^D; r^D\}$.

V. Results

In this section, the driver-in-the-loop experiment results are presented. Two driver performance predictors, ED and ANFIS, are compared. In this paper, the performance results of only one driver are introduced and are studied in detail. A random driver was selected from the group of driver-in-the-loop experiment participants. For all other drivers, the results are very similar.

A. A comparison between ED and ANFIS predictors

In Fig. 11, a comparison between ED calculation and ANFIS predictors is reported. The red curve symbolizes performance prediction by the ED, whereas the blue curve – prediction by the ANFIS. Predicted results obtained from the ED and the ANFIS are similar for both Δv_p (Fig. 11 a) and Δx_p (Fig. 11 b).

The main difference between the prediction algorithms is that the ANFIS comparing to the ED has a smooth output. Nevertheless, the average prediction accuracy is almost the same for both algorithms. It can be explained by the ANFIS hybrid training algorithm, where both antecedent and consequent parameters are optimized in the backward and forward passes, respectively [38]. The ED predictor, however, has higher oscillation. The algorithm uses only the preprocessed data with a single simplification. It provides slightly more

TABLE IV
ANFIS and ED Prediction Accuracy Comparison

Predictor	Δv_{RMSE} [km/h]	Δx_{RMSE} [m]	t_{train} [s]
ANFIS	2.1345	0.1506	148.072
ED	1.9992	0.1405	96.150

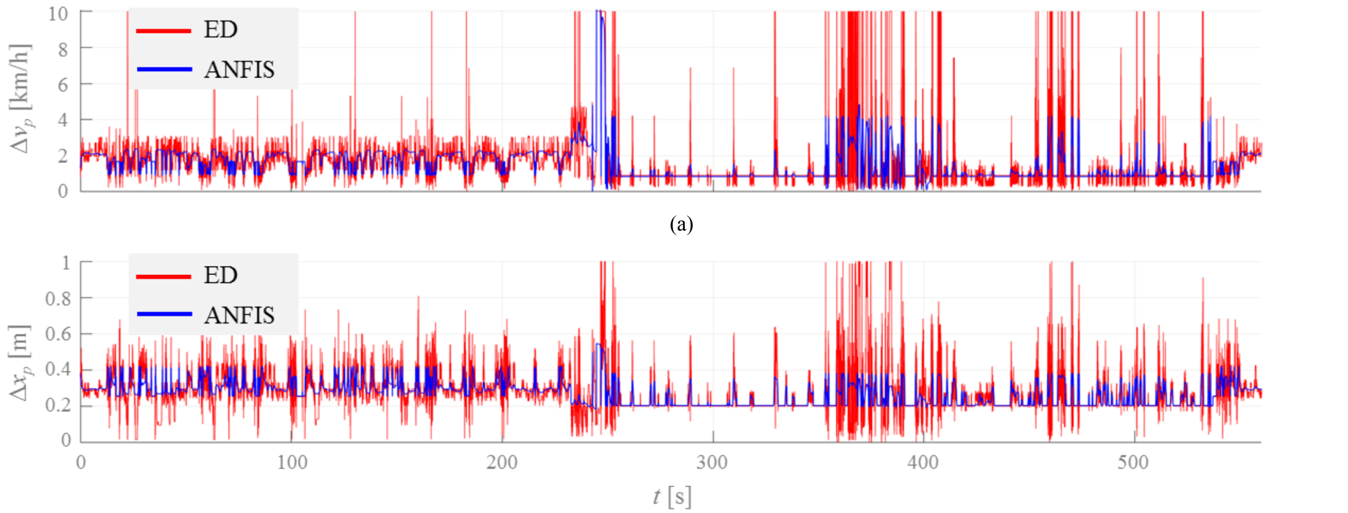

(b)

Fig 11. Driver performance prediction algorithms comparison: the red curve represents performance prediction by the ED; the blue curve displays performance prediction by the ANFIS: (a) Δv_p; (b) Δx_p.

accurate prediction and, though, frequent fluctuation. Nevertheless, the output response remains identical to the ANFIS.

In Table IV, the root mean squared errors, which are responsible for algorithm prediction accuracy, for every predicted variable, Δv_{RMSE} and Δx_{RMSE}, are reported. In addition, the algorithms' training time t_{train} is calculated. The ED shows more accurate prediction capabilities and faster training term comparing to the identical ANFIS predictor. For the rest of the Section only the ED predictor results are studied.

B. DD detection

Fig. 12 demonstrates driving performance of one of the experiment participants conducting a secondary task. The gray background symbolizes a period of the secondary distractive activity (i.e. the cellular telephone is in the driver's hand). Red lines on every plot mark the predicted performance, namely speed limit maintenance (Fig. 12 a) and lane keeping ability (Fig. 12 b). Black line is driver's real performance. Green curves represent an appropriate information about the road segment (Fig. 9): speed limit (Fig. 12 a) and curvature (Fig. 12 b). The small road radius designates a sharp turn, while the big radius – almost straight road.

It is observed that the driver failed in holding optimal speed limits (Fig. 12 a) while performing the secondary activity. The method predicted that the driver would not surpass the difference between actual and optimal for the road speeds in 3 km/h on most of the road segments. Nevertheless, the participant being distracted decreased or increased the vehicle velocity by more than 5 km/h relatively the road speed limit.

For the studied driver, the speed limit maintenance on the 50 km/h speed limit segment was harder than on a high speed limit (i.e. 90 km/h) one (Fig. 12 a). The road is significantly curvy on the low speed road part, whereas the high speed limit segment is almost straight (Fig. 9; Fig. 12 b). This is also predicted by the ED (Fig. 12 a).

The driver faced difficulties keeping the vehicle in the middle

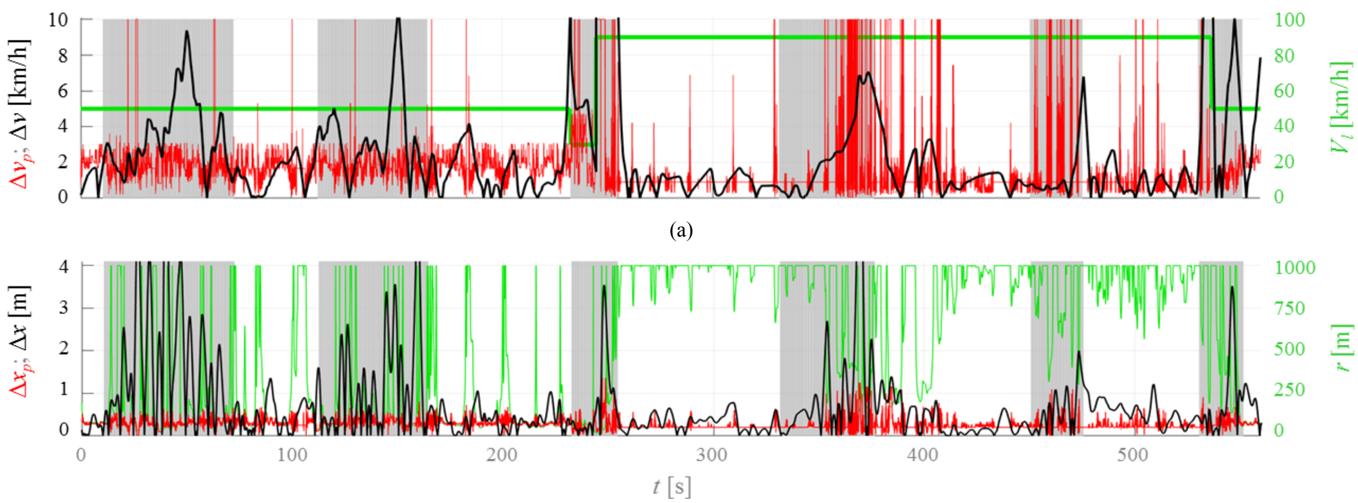

(b)

Fig 12. Driver performance prediction versus real driver performance example: gray background – the secondary task accomplishment period; black curve – real driver performance; red curve – predicted driver performance by the ED calculation; green curve – information about the road segment: (a) Δv_p, Δv, and V_l; (b) Δx_p, Δx, and r.

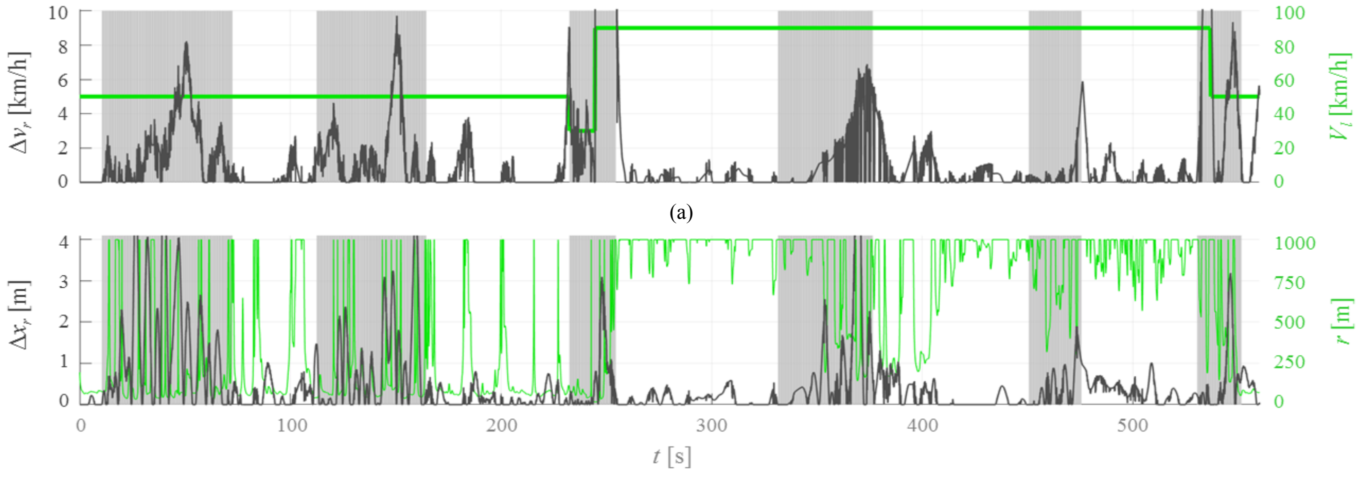

Fig 13. Resultative driver performance with ED predictor: gray background – the secondary task accomplishment period; dark gray curve – driver resultative performance (Eq. (2), (3)); green curve – information about the road segment: (a) Δv_r and V_l; (b) Δx_r and r.

of the lane while performing the secondary task (Fig. 12 b). In some moments, the driver went more than 4 m far from the centerline. The width of the modeled in the virtual world vehicle is 1.5 m. The width of a single lane is 3.5 m. It means that when Δx is higher than 1 m, the participants drive outside the lane bounds. Although, the ED predicts that the driver's Δx does not exceed 0.5 m while normal performance, the Δx was higher than 1 m when the driver interacted with the mobile phone. Hence, the driver always drove off the road while chatting on a cell phone. Consequently, by applying the methods of the prediction of driver performance, an abnormal driver's behavior may be recognized. As this behavior is caused by the secondary task accomplishment, it can be concluded that the method is suitable for DD detection.

In Fig. 13, the resultative driver performance diagrams are acquainted. The response values were calculated applying (2) and (3) for the ED predictor. The results help estimate the difference between driving with the secondary task and normal driving from the viewpoint of the speed limit maintenance and the lane keeping ability. Both estimates, Δv_r and Δx_r, have similar levels: low at normal driving and significantly high while performing the secondary task.

C. DD evaluation

In Fig. 14, a percentage level of DD is shown. The curve represents the result of the FL data fusion. Two variables, Δv_r and Δx_r (Fig. 13), pass through FL evaluator. The prediction method represents normal driving (Fig. 14, white background) for each individual participant, when evaluation of the driving performance does not exceed 20%. On the contrary, when the driver performs secondary task, her/his lane keeping and speed maintenance ability degrade. The algorithm easily detects this phenomenon and FL evaluates driving performance with significantly high percentage (Fig. 14, gray background).

DD remains still high in a few seconds after secondary task accomplishment (Fig. 14) because the drivers, after completing the distractive task, realize the errors and try to return to their lane and increase/decrease the speed as soon as possible. This maneuver causes additional mistakes in vehicle operation. Thus, DD is often dangerous not only during the secondary activity execution, but also for few seconds after. Hence, the secondary activity increases the period of distraction.

Using the proposed method and considering 20% of DD as abnormal driving, it can be seen in Fig. 14 that the driver was always distracted while interacting with the mobile phone. The experiment results are also confirmed by the driver-in-the-loop experiment participants' subjective evaluation. All the drivers mentioned that they experienced visual, biomechanical, and cognitive distractions at the same time, what caused their driving performance burden leading to abnormal driving. This phenomenon was assured by the proposed method (Fig. 14).

Furthermore, although the participants were informed about the experiment procedure in details, and they were able to observe their position on a track on one of the SEP screens, it did not help them to avoid distraction induced by the interaction with cell phones (Fig. 14). It also proves the statement from [3]: *"our cognitive ability does not allow us to engage in more than*

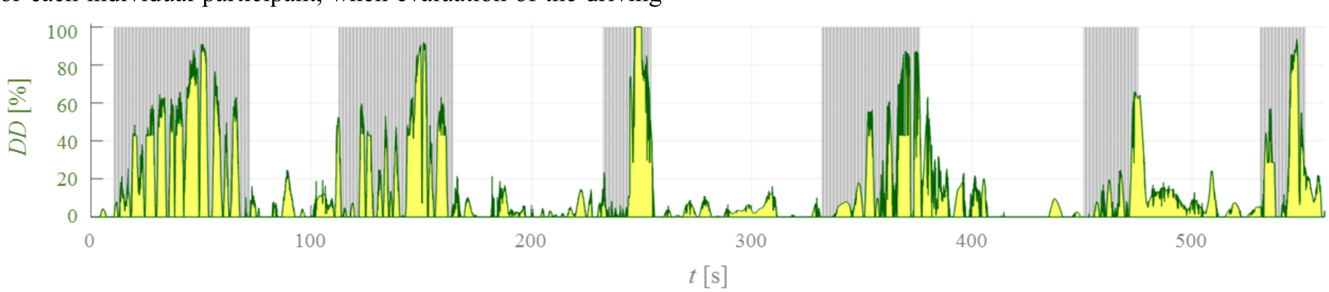

Fig 14. DD evaluation: gray background – the secondary task accomplishment period; green-yellow curve – *DD* detected with the ED predictor.

one conscious task simultaneously." It certifies that when the driver is involved in the secondary activity, safe driving is not guaranteed. Thus, minimization of DD is worthy of significant effort and work.

VI. Conclusion

This paper presents a method for DD detection and evaluation while performing a secondary task. The detection is executed by the machine learning algorithm based on the ED calculation formula. FL fuses the performance-based data to evaluate a level of DD in percentages. The main contribution of this work is solving a regression problem in DD detection and performance-based data fusion into a single variable introduced for the DD assessment. Therefore, the method is capable not only to detect DD, but also to evaluate its influence on safe driving performance.

A machine learning algorithm predicts driver performance in a name of lane keeping and speed maintenance ability on a specific road segment. A road segment is described by speed limit and road curvature. The data used in machine learning are collected during driver's normal performance, when no distraction activity appears. To recognize DD, the proposed method compares distracted while conducting a secondary task driving with normal one, free from distraction, performances.

To verify the proposed DD detection and evaluation method, the driver-in-the-loop experiment on driving decoy performing a secondary task with 18 participants was conducted. Chatting on a cellular telephone is examined as a secondary task. Data collected during two full laps driving is exploited for predictor design. One more lap is driven with a secondary activity execution. The proposed method enables accurate driver decoy experimentation. The results presented in this paper prove that the proposed method is capable to detect and to measure precisely the percentage level of DD caused by an unusual driver performance. The methodology is adaptable to each individual driver. It allows examination and comparison of the secondary tasks influence on driving quality of various drivers.

The suggested methodology has a certain advantage over other DD detection methods described in Section II. Particularly, as compared to the methods, where the behavioral and psychological attributes are applied [6-18], the proposed approach does not require additional devices, such as cameras and neuroscan systems. Those devices increase the system cost [8], what in its turn is a potential resistance for system application in a commercial passenger vehicle. For the same reason, the methods with different attribute combinations (e.g. behavioral, psychological, and subjective) [30-35] are not feasible in the real world implementation.

The method introduced here, like in [2, 20-27], uses only performance-based attributes, because the variables can be obtained using the data from the available in modern vehicles sensors [19]. However, the method described here, in comparison with other performance-based approaches and with all the works mentioned in Section II, is able to measure a level of DD. The nonlinear regression technique used for DD detection gives an opportunity for a precise DD measurement. On the contrary, all the previously proposed methods are binary classifiers with Boolean output (distracted/non-distracted). Consequently, the suggested method can be used as a practical tool for different evaluation and comparative analyses of the secondary tasks influence on vehicle safety.

This work, however, has several limitations. Exactly, it misses a statistical analysis with a greater sample size of different driver segments (e.g. distributed between age, gender, driving experience, etc.). This analysis will be conducted in the future works. What is more, in this paper, the case study involved only one secondary task: texting on a cell phone. In the future, a variety of different DD activities will be tested on their influence of the DD level. Like in [33], the IVIS will be exploited as a number of secondary activities. To this regard, the experiments will be conducted on the advanced vehicle mockup with a vehicle cockpit identical to the one used in commercial vehicles. Finally, the method will be also extended to more driving-performance variables, and different DD recognition attributes will be combined.

Acknowledgment

The authors would like to thank IPG Automotive GmbH (Karlsruhe, Germany) for providing the test rig. We extend our special thanks to the volunteers from IPG Automotive GmbH for participating in the driver-in-the-loop experiment.

References

[1] M. Westin, R. Dougherty, C. Depcik, A. Hausmann, and C. Sprouse III, "Development of an adaptive-human-machine-interface to minimize driver distraction and workload," in *Proc. in the ASME 2013 Int. Mechan. Engin. Cong. and Expos.*, San Diego, California, USA, 2013, pp. 1-13.

[2] T. Ersal, H. J. A. Fuller, O. Tsimhoni, J. L. Stein, and H. K. Fathy, "Model-based analysis and classification of driver distraction under secondary tasks," *IEEE Trans. on Intel. Transp. Syst.*, vol. 11, no. 3, pp. 692-701, Sept. 2010.

[3] National Traffic Law Center. Investigation and prosecution of distracted driving cases. Report no. DOT HS 812 407. Washington, DC: National Highway Traffic Safety Administration, 2017.

[4] Y. Liang, J. D. Lee, and M. L. Reyes, "Nonintrusive detection of driver cognitive distraction in real time using Bayesian networks," *Transp. Research Rec.: Jour. of the Transp. Research Board*, vol. 2018, 2007, pp. 1-8, Dec. 2007.

[5] T. Liu, Y. Yang, G.-B. Huang, Y. K. Yeo, and Z. Lin, "Driver distraction detection using semi-supervised machine learning," *IEEE Trans. on Intel. Transp. Syst.*, vol. 17, no. 4, pp. 1108-1120, April 2016.

[6] S. Wang, Y. Zhang, C. Wu, F. Darvas, and W. A. Chaovalitwongse, "Online prediction of driver distraction based on brain activity patterns," *IEEE Trans. on Intel. Transp. Syst*., vol. 16, no. 1, pp. 136-150, Feb. 2015.

[7] J. Jo, S. J. Lee, H. G. Jung, K. R. Park, and J. Kim, "Vision-based method for detecting driver drowsiness and distraction in driver monitoring system," *Optic. Engin*., vol. 50, no. 12, pp. 1-24, Dec. 2011.

[8] C. Ahlstrom, K. Kircher, and A. Kircher, "A gaze-based driver distraction warning system and its effect on visual behavior," *IEEE Trans. on Intel. Transp. Syst*., vol. 14, no. 2, pp. 965-973, June 2013.

[9] X.-P. Huynh, S.-M. Park, and Y.-G. Kim, "Detection of driver drowsiness using 3D deep neural network and semi-supervised gradient boosting machine," in *Asian Conf. on Comp. Vision (ACCV), Lecture Notes in Computer Science*, vol 10118. Springer, 2016, pp. 134-145.

[10] L. Fridman, P, Langhans, J, Lee, and B. Reimer, "Driver gaze region estimation without use of eye movement," *IEEE Intel. Syst*., vol. 31, no. 3, pp. 49-56, May 2016.

[11] I.-H. Choi, S. K. Hong, and Y.-G. Kim, "Real-time categorization of driver's gaze zone using the deep learning techniques," in *2016 Intern. Conf. on Big Data and Smart Comp. (BigComp)*, Hong Kong, China, 2016, pp. 143-148.

[12] A. Azman, S. Z. Ibrahim, Q. Meng, and E. A. Edirisinghe, "Physiological measurement used in real time experiment to detect driver cognitive distraction," in *2014 Intern. Conf. on Electr., Inform. and Commun. (ICEIC)*, Kota Kinabalu, Malaysia, 2014, pp. 1-5.

[13] P. Jiménez, L. M. Bergasa, J. Nuevo, N. Hernández, and I. G. Daza, "Gaze fixation system for the evaluation of driver distraction induced by IVIS," *IEEE Trans. on Intel. Transp. Syst*., vol. 13, no. 3, pp. 1167-1178, Sept. 2012.

[14] M.-H. Sigari, M. Fathy, and M. Soryani, "A driver face monitoring system for fatigue and distraction detection," *Intern. Jour. of Vehic. Techn., vol. 2013*, pp. 1-11, Jan. 2013.

[15] Y. Jiao, Y. Peng, B.-L. Lu, X. Chen, S. Chen, and C. Wang, "Recognizing slow eye movement for driver fatigue detection with machine learning approach," in *2014 Intern. Joint Conf. on Neural Netw. (IJCNN)*, Beijing, China, 2014, pp. 4035-4041.

[16] H. Matsuo, and A. Khiat, "Prediction of drowsy driving by monitoring driver's behavior," in *21st Intern. Conf. on Pattern Recogn. (ICPR 2012)*, Tsukuba, Japan, 2012, pp. 3390-3393.

[17] V. Alizadeh and O. Dehzangi, "The impact of secondary tasks on drivers during naturalistic driving: Analysis of EEG dynamics," in *2016 IEEE 19th Intern. Conf. on Intell. Transp. Syst. (ITSC)*, Rio de Janeiro, Brazil, 2016, pp. 2493-2499.

[18] M. Babaeian, N. Bhardwaj, B. Esquivel, and M. Mozumdar, "Real time driver drowsiness detection using a logistic-regression-based machine learning algorithm," in *2016 IEEE Green Ener. and Syst. Conf. (IGSEC)*, Long beach, CA, USA, 2016, pp. 1-6.

[19] E. Zabler, "Sensors for Brake Control", in K. Reif, *Brakes, Brake Control and Driver Assistance Systems: Function, Regulation and Components.* Wiesbaden, Germany: Springer Vieweg, 2014, pp. 142-153.

[20] S. Qiu, R. McGee, and Y. L. Murphey, "Adaptive fuzzy prediction for automotive application usage," in *2015 IEEE 14th Intern. Conf. on Mach. Learn. and Applic. (ICMLA)*, Miami, FL, USA, 2015, pp. 19-24.

[21] SJ. Choi, JH. Kim, DG. Kwak, P. Angkititrakul, and J. H. L. Hansen, "Analysis and classification of driver behavior using in-vehicle CAN-bus information," in *2011 IEEE Intern. Conf. on Multim. and Expo (ICME)*, Barcelona, Spain, 2011, pp. 1-6.

[22] S. Im, C. Lee, S. Yang, J. Kim, and B. You, "Driver distraction detection by in-vehicle signal processing," in *2014 IEEE Symp. on Comput. Intel. in Vehic. and Transp. Syst. (CIVTS)*, Orlando, FL, USA, 2015, pp. 1-5.

[23] J. Yang, T. N. Chang, and E. Hou, "Driver distraction detection for vehicular monitoring," in *IECON 2010 - 36th Annual Conf. on IEEE Indust. Electron. Soc.*, Glendale, AZ, USA, 2010, pp. 108-113.

[24] V. Martínez, I. del Campo, J. Echanobe, and K. Basterretxea, "Driving behavior signals and machine learning: A personalized driver assistance system," in *2015 IEEE 18th Intern. Conf. on Intel. Transp. Syst.*, Las Palmas, Spain, 2015, pp. 2933-1940.

[25] T. Kumagai and M. Akamatsu, "Prediction of human driving behavior using dynamic Bayesian network," *IEICE Trans. on Infrom. and Syst*., vol. E89-D, no. 2, pp. 857-860, Feb. 2006.

[26] C. Miyajima and K. Takeda, "Driver-behavior modeling using on-road driving data." *IEEE Sign. Proc. Soc.*, vol. 33, no. 6, pp. 14-21, Nov. 2015.

[27] F. Tango and M. Botta, "Real-time detection system of driver distraction using machine learning," *IEEE Trans. on Intel. Transp. Syst.*, vol. 14, no. 2, pp. 894-905, June 2013.

[28] M. Miyaji, H. Kawanaka, and K. Oguri, "Study on effect of adding pupil diameter as recognition features for driver's cognitive distraction detection," in *2010 7th Intern. Symp. on Communi. Syst., Netw. & Digit. Signal Proc. (CSNDSP 2010)*, Newcastle upon Tyne, UK, 2010, pp. 1-6.

[29] P. Hermannstädter and B. Yang, "Driver distraction assessment using driver modeling," in *2013 IEEE Intern. Conf. on Syst., Man, and Cyber*., Manchester, UK, 2013, pp. 3693-3698.

[30] Y. Liao, S. E. Li, W. Wang, Y. Wang, G. Li, and B. Cheng, "Detection of driver cognitive distraction: A comparison study of stop-controlled intersection and speed-limited highway," *IEEE Trans. on Intel. Transp. Syst.*, vol. 17, no. 6, pp. 1628-1637, June 2016.

[31] Y. Liang, M. L. Reyes, and J. D. Lee, "Real-time detection of driver cognitive distraction using support vector machines," *IEEE Trans. on Intel. Transp. Syst.*, vol. 8, no. 2, pp. 340-350, June 2007.

[32] C. Schwarz, T. Brown, J. Lee, J. Gaspar, and J. Kang, "The detection of visual distraction using vehicle and driver-based sensors," in *Proc. SAE Technical Paper*, April 2016, doi:10.4271/2016-01-0114.

[33] M. Wöllmer, C. Blaschke, T. Schindl, B. Schuller, B. Färber, S. Mayer, and B. Trefflich, "Online driver distraction detection using long short-term memory," *IEEE Trans. on Intel. Transp. Syst*., vol. 12, no. 2, pp. 574-582, June 2011.

[34] F. Tango, C. Calefato, L. Minin, and L. Canovi, "Moving attention from the road: A new methodology for the driver distraction evaluation using machine learning approaches," in *2009 2nd Conf. on Human Syst. Interact.*, Catania, Italy, 2009, pp. 596-599.

[35] C. Craye, A. Rashwan, M. S. Kamel, and F. Karray, "A multi-modal driver fatigue and distraction assessment system," *Intern. Jour. of Intel. Transp. Syst. Research*, vol. 14, no. 3, pp. 173-794, Sep. 2016.

[36] E. Alpaydin, *Introduction to Machine Learning*. Cambridge, Massachusetts: USA: The MIT Press, 2004, pp. 105-132.

[37] K. M. Passino and S. Yurkovich, *Fuzzy Control*. California: USA: Addison Wesley, 1998.

[38] M. Negnevitsky, *Artificial Intelligence: A Guide to Intelligent System*. 2nd ed. Harlow, England: Adison-Wesley, 2005, pp. 259-300.

[39] A. Aksjonov, P. Nedoma, V. Vodovozov, E. Petlenkov, and M. Herrmann, "A method of driver distraction evaluation using fuzzy logic," in *2017 XXVI Intern. Conf. on Inform., Commun. and Autom. Techn. (ICAT)*, Sarajevo, Bosnia & Herzegovina, 2017, pp. 23-28.

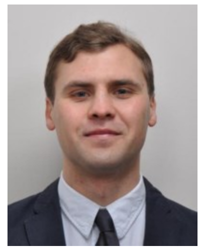

Andrei Aksjonov received his B.Sc. and M.Sc. in electrical engineering and electrical drives and power electronics with automation specialization from Tallinn University of Technology in 2013 and 2015, respectively. He is currently a Marie Skłodowska-Curie research fellow hosted by Škoda Auto a.s. His research topic is the development of driver distraction detection and human-machine interface evaluation methods for multi-actuated ground vehicles. His research interests include HMI, fuzzy systems, machine learning, vehicle safety, ADAS.

Pavel Nedoma received his M.Sc. and Ph.D. from Czech Technical University in Prague in 1985 and 2007, respectively. Since 1985, he has been working at the ŠKODA AUTO Concept Development Department as a Development Engineer. He is responsible on development experimental tools for simulation, supervision, analysis, processing and visualization HMI interaction between driver and other on-board systems, HMI measurements in car ride simulators and comparative measurements performed in real vehicles.

Valery Vodovozov (M'-) received his Candidate of Science degree and Associate Professor and Senior Researcher academic titles in Electrical Engineering from St. Petersburg Electrotechnical University, Russia. He is a professor of Tallinn University of Technology, Estonia, a member of IEEE, International Institute of Informatics and Systemics (IIIS), and Global Research Alliance of Texas Institute of Science (TxIS GRA). His research interests include power electronics and electrical drives areas.

Eduard Petlenkov received his B.Sc., M.Sc. and Ph.D. degrees in computer and systems engineering from Tallinn University of Technology. He is professor in the Department of Computer Systems at Tallinn University of Technology. His main research interests lie in the domain of nonlinear control, system analysis and computational intelligence.

Martin Herrmann received his B.Sc. and M.Sc. in automotive engineering from Ilmenau University of Technology in 2012 and 2014. He is currently Business Development Manager at IPG Automotive focusing on methods for testing ADAS and automated driving functions in virtual environments. This includes especially road, traffic and sensor modeling.